Decrease of renal aquaporins 1-4 is associated with renal function impairment in pediatric congenital hydronephrosis

Zhen-Zhen Li, Lu Xing, Zhan-Zheng Zhao, Jin-Sheng Li, Rui Xue, Avinash Chandra, Rikke Nørregaard, Jian-Guo Wen

Zhengzhou, China

Background: **Renal aquaporins (AQP1-4) concentration is downregulated and is in proportion to the degree of hydronephrosis graded by ultrasound in pediatric congenital hydronephrosis (CH). However, the relationship between the expression of AQP1-4 with the changes of renal function impairment (RFI) evaluated by ^{99m}Tc-DTPA renal dynamic imaging is still unclear. This study aimed to investigate the relationship between AQP1-4 expression and degree of RFI in children with CH.**

Methods: **The expression of AQP1-4 was evaluated in 45 children with unilateral ureteropelvic junction obstruction (28 boys and 17 girls, average age: 28±10 months) and 15 children undergoing nephrectomy for nephroblastoma (8 boys and 7 girls, average age: 26±8 months) by immunoblotting and immunohistochemistry. Renal function was graded into mild and severe RFI by ^{99m}Tc-DTPA renal dynamic imaging.**

Results: **One-way analysis of variance with Bonferonni's correction showed a significantly reduced protein expression of AQP1-4 in the severe RFI group compared with those in both mild RFI group and controls (AQP1: 0.52±0.09 *vs.* 0.91±0.06 *vs.* 1.23±0.033; AQP2: 0.68±0.12 *vs.* 1.09±0.06 *vs.* 1.52±0.08; AQP3: 0.59±0.16 *vs.* 0.94±0.08 *vs.* 1.31±0.07; AQP4: 0.64±0.06 *vs.* 1.14±0.07 *vs.* 1.61±0.07; *P*<0.001, respectively). In kidneys with severe RFI, there was a reduction in the protein concentration of all four AQP isoforms which was more pronounced compared with those seen in kidneys with mild RFI and in the controls.**

Conclusion: **AQP1-4 expression is reduced in proportion with the impairment degree of renal function graded by ^{99m}Tc-DTPA renal dynamic imaging in human CH.**

World J Pediatr 2012;8(4):335-341

Key words: **aquaporins; congenital hydronephrosis; renal function; ^{99m}Tc-DTPA renal dynamic imaging**

Original article

Introduction

Recently, animal studies have revealed that the expression of aquaporins (AQPs) was long-term downregulated in response to either unilateral or bilateral ureteral obstruction,[1-4] also shown that dysregulation of AQPs may contribute to the impairment of urinary concentrating capacity associated with obstructive nephropathy. We found that the expression of AQP1-4 mRNA and protein concentration was also downregulated and it was in proportion to the degree of hydronephrosis graded by ultrasound in pediatric congenital hydronephrosis (CH).[5] However, the relationship between the expression of AQP1-4 with the change of renal function impairment (RFI) evaluated by ^{99m}Tc-DTPA renal dynamic imaging is still unclear.

The most popular tools used in evaluation of CH are ultrasonography and ^{99m}Tc-DTPA renal dynamic imaging. Ultrasonography is the simplest and noninvasive technique for the detection of urinary tract dilation,[6] but it can not provide the detailed information about renal function in the obstructed kidney. At present, ^{99m}Tc-DTPA renal dynamic

Author Affiliations: The Institute of Clinical Medicine (Li ZZ, Xing L, Li JS, Xue R, Chandra A, Wen JG), Pediatric Urodynamic Center, Urology Department (Xing L, Li JS, Wen JG), Nephrology Department (Zhao ZZ), and Neurology Department (Chandra A), First Affiliated Hospital of Zhengzhou University, Zhengzhou, China; The Water and Salt Research Center, Institute of Clinical Medicine, Aarhus University, Aarhus, Denmark (Nørregaard R)

Corresponding Author: Jian-Guo Wen, MD, PhD, The Pediatric Urodynamic Center, Urology Department of First Affiliated Hospital of Zhengzhou University, The Institute of Clinical Medicine Universities, Zhengzhou 450052, China (Tel: +86-371-66295219; Fax: +86-371-66989950; Email: jgwen@zzu.edu.cn)

doi: 10.1007/s12519-012-0378-9

imaging as the gold standard is used most commonly to evaluate renal function in clinical practice.[7,8] Therefore, it is possible to explore the relationship between downregulation of AQP1-4 and renal function evaluated by ^{99m}Tc-DTPA renal dynamic imaging.

The purpose of the present study was to investigate the relationship between the AQP1-4 expressions in CH caused by ureteropelvic junction obstruction (UPJO) with different renal function impairment demonstrated by ^{99m}Tc-DTPA renal dynamic imaging.

Methods

Patients

Renal tissue samples (50 to 80 mg each) were harvested from 45 kidneys (26 left and 19 right kidneys) in 28 boys and 17 girls (28±10 months old) who underwent unilateral Anderson-Hynes pyeloplasty due to UPJO in the First Affiliated Hospital of Zhengzhou University, China from November 2008 to December 2010. All the samples were collected during surgical intervention. All patients had a prenatal diagnosis of unilateral hydronephrosis during routine fetal ultrasound, and a postnatal examination reconfirmed the diagnosis of UPJO. All patients were evaluated before pyeloplasty by abdominal ultrasound and ^{99m}Tc-DTPA renal dynamic imaging. Exclusion criteria were associated anomalies, including vesicoureteral reflux, ureterovesical junction obstruction and posterior urethral valves obstruction, bilateral hydronephrosis, previous operation on the urinary system and other deformations of the external genital organs, deformations in the lower part of the ureter, bladder, and urethra, urinary stones, neurogenic bladder dysfunction, and "supranormal function" of the affected kidney (DRF >55%). The Ethical Committee of the Zhengzhou University Hospital. Consent was obtained from the parents of the children.

Renal control samples were obtained from 15 patients (8 boys and 7 girls, average age: 26±8 months) who accepted nephrectomy for nephroblastoma and were confirmed histologically to be normal. Part of the renal tissue specimen stored at -80°C was available for immunoblotting or fixed in 10% neutral buffer formalin for immunohistochemistry.

^{99m}Tc-DTPA renal dynamic imaging

An injection of ^{99m}Tc-DTPA (Technescan DTPA; Mallinckrodt Medical, Hazelwood, MO, USA) was given and the dose was 5 MBq/kg for body weight under 20 kg (minimum 50 MBq) and 4 MBq/kg for body weight more than 20 kg according to the method described by Gutte et al.[9] Posterior imaging of the children in the supine position was collected using a large-field-of-view dual-head gamma camera (HawKeye VG5 SPECT/CT, GE, USA).

According to the reported results,[10] 30 cases of CH had mild RFI and 15 had severe RFI. The evaluative standard of renal function impairment was based on the shape of the time activity curve (TAC) and time of peak (TOP) in ^{99m}Tc-DTPA renal dynamic imaging. The mild RFI group showed parabolic TAC (section a was normal or slightly lower, section b was normal or rose slowly and section c was slowing down or continued rising) (Fig. 1A) and the TOP was 6.036±2.293 minutes (mean ± SD), whereas the severe RFI group showed high or low level extension cord in TAC (section a was

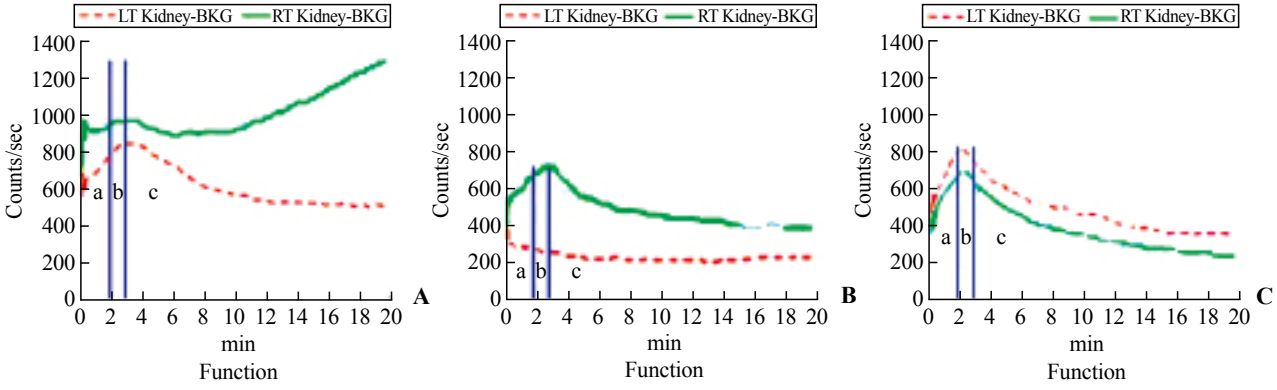

Fig. 1. ^{99m}Tc-DTPA renal scintigraphy renogram in the hydronephrotic and control kidneys. **A:** Representative mild renal function impairment (RFI) group: ^{99m}Tc-DTPA renal scintigraphy renography showed parabolic time-activity curves; section a was normal or slightly lower, section b was normal or rose slowly and section c was slow down or continued rising. Top to peak (TOP) was 2.72 in the left kidney, and 19.72 in the right kidney; **B:** Representative severe RFI group: ^{99m}Tc-DTPA renal scintigraphy renography showed high or low level extension cord in time-activity curve; section a was normal or slightly lower, section b and c fused and formed an extension cord. TOP was 1.24 in the left kidney, and 2.74 in the right kidney; **C:** Representative renal control group: ^{99m}Tc-DTPA renal scintigraphy renography showed normal time-activity curves; section a, b and c were of normal shape. TOP was 2.17 in the left kidney, and 2.17 in the right kidney.

normal or slightly lower, section b and c fused and formed an extension cord) (Fig. 1B) and the TOP was 19.213±0.776 minutes. The renal control group showed normal TAC (section a, b and c were normal shape) (Fig. 1C) and the TOP was 2.555±0.242 minutes.

Electrophoresis and immunoblotting

Total protein was prepared from tissue samples. Tissues (10 mg) were lysed in 200 μL Tissue Protein Extraction Reagent (Sigma-Aldrich Co. CelLytic MT 50 mL, USA) and homogenized. The lysate was then centrifuged at 12 000 rpm for 15 minutes to pellet tissue debris. Protein concentration was determined using the Bio-Rad protein assay kit (Bio-Rad, Hercules, CA, USA). For each sample, protein extract (100 μg) was loaded and separated with Sodium Dodecyl Sulfate-Polyacrylamide Gel Electrophoresis consisting of a 12% polyacrylamide resolving gel and a 4% polyacrylamide stacking gel. The proteins were electrophoretically transferred to a nitrocellulose membrane. The membranes were stained with 0.1% Coomassie blue to check the efficiency of the transfer. Unstained membranes were washed with Tris-buffered saline (pH 7.4) containing 0.1% Tween-20 (TBST) and blocked for 1 hour with 5% nonfat milk in TBST. The membranes were then incubated overnight at 4ºC with affinity-purified, anti-rabbit polyclonal antibodies against AQP1 (1:200), AQP2 (1:200), AQP3 (1:200), and AQP4 (1:200, Santa Cruz Biotechnology, Santa Cruz, CA, USA), in TBST with 5% nonfat milk. Mouse anti-rabbit IgG monoclonal antibody concentration of 1:8000 (Zhongshan Biotechnology, Beijing, China) was used to incubate the membrane for one hour at room temperature, upon which the membrane was washed in TBS. The bound antibody was detected by enchanced chemiluminescence (ECL) technology (Amersham, UK). β-actin (1:200, Santa Cruz Biotechnology, Santa Cruz, CA, USA) reacted with the same samples as an internal control. ECL films were scanned using a Hewlett-Packard Scanjet scanner and Adobe Photoshop software. For each sample, densitometric analysis of immunoblotting was performed with the use of ImageJ imaging processing software. The labeling density of blots was determined from samples of kidneys of mild RFI, severe RFI and normal control groups. The labeling density was corrected by densitometry of β-actin. Measurements were expressed as arbitrary units.

Immunohistochemical analysis

The protein expression of AQP1-4 was assessed by immunohistochemical analyses using an immunoperoxidase procedure. Kidney samples were processed for immunohistochemistry by means of standard techniques. The sample tissue was fixed in 4% buffered formaldehyde and embedded in wax. The paraffin-embedded tissues were cut at 2 μm on a rotary microtome (Leica). The sections were dewaxed and rehydrated. For immunoperoxidase labeling, endogenous peroxidase was blocked by 0.5% H_2O_2 in absolute methanol for 10 minutes at room temperature. To reveal antigens, the sections were put in 1 mmol Tris solution (pH 9.0) supplemented with 0.5 mmol EDTA and heated in a microwave oven at 650W for 6 minutes and then at 350W for 10 minutes. After the treatment, the sections were left for 30 minutes in the buffer for cooling. Nonspecific binding of IgG was prevented by incubating the sections in 50 mmol NH4CL for 30 minutes, followed by blocking in phosphate buffered saline (PBS) supplemented with 1% bovine serum albumin (BSA), 0.05% saponin, and 0.2% gelatin. The sections were incubated overnight at 4ºC with primary antibodies rabbit anti-AQP1-4 (Santa Cruz Biotechnology, Santa Cruz, CA, USA) diluted in PBS supplemented with 0.1% BSA and 0.3% Triton X-100. They were rinsed with PBS supplemented with 0.1% BSA, 0.05% saponin, and 0.2% gelatin and then incubated with horseradish peroxidase-conjugated secondary antibody (P448, diluted 1:200, DAKO). Labeling was visualized by 0.05% 3, 3 diaminobenzidine tetrahydrochloride (DAB). Microscopy was carried out using a Leica DMRE light microscope. The sections taken from normal kidney and CH tissue were labeled at the same time with the same solutions to allow for comparison. Negative controls for immune-specificity were included in all experiments with PBS, using matching concentrations of normal rabbit serum

Statistical analysis

The Statistical Program for Social Sciences, version 13.0 (SPSS, Chicago, Ill), was used for statistical analysis. Results were expressed as mean ± SD. $P<0.05$ was considered statistically significant. One-way analysis of variance (ANOVA) with Bonferonni's correction was used to compare AQP1-4 levels between the groups.

Results

Immunoblotting of AQP1-4 showed that there was a gradual reduction in the protein abundance of all 4 aquaporins in proportion with the degree of RFI as compared with the control kidney tissues (Fig. 2). In the severe RFI group, the protein expression of AQP1-4 was significantly reduced compared with both control

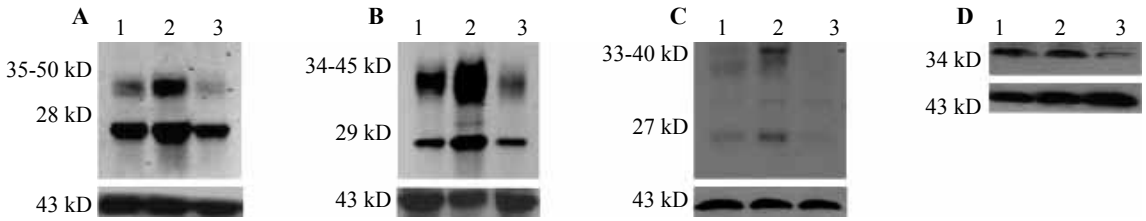

Fig. 2. Semi-quantitative immunoblots of aquaporins (AQP) 1-4 using kidney protein isolated from kidney tissue samples. A total of 100 μg proteins were used to assay the different AQPs in the renal control group (lane 2), mild renal function impairment (RFI) group (lane 1) and severe RFI group (lane 3). **A:** Immunoblots were reacted with anti-AQP1 and revealed a 28-kDa and 35 to 50-kDa bands, representing nonglycosylated and glycosylated form of AQP1 (upper panel) and 43 kDa band representing β-actin (lower panel); **B:** Immunoblots were reacted with anti-AQP2 and revealed a 29-kDa and 35 to 45-kDa bands, representing nonglycosylated and glycosylated form of AQP2 (upper panel) and 43kDa band representing β-actin (lower panel); **C:** Immunoblots were reacted with anti-AQP3 and revealed a 27-kDa and 35 to 40-kDa bands, representing nonglycosylated and glycosylated form of AQP3 (upper panel) and 43 kDa band representing β-actin (lower panel); **D:** Immunoblots were reacted with anti-AQP4 and revealed a 34-kDa, representing nonglycosylated form of AQP4 (upper panel) and 43 kDa band representing β-actin (lower panel).

Table. Expression of aquaporins (AQP) 1-4 protein in patients with congenital hydronephrosis and normal controls (mean±SD)

Aquaporin	Normal control (n=15)	Mild RFI group (n=30)	Severe RFI group (n=15)
AQP1	1.23 ± 0.03*†	0.91 ± 0.06‡	0.52 ± 0.09
AQP2	1.52 ± 0.08*†	1.09 ± 0.06‡	0.68 ± 0.12
AQP3	1.31 ± 0.07*†	0.94 ± 0.08‡	0.59 ± 0.16
AQP4	1.61 ± 0.07*†	1.14 ± 0.07‡	0.64 ± 0.06

*: P<0.001, *vs.* mild RFI group; †: P<0.001, *vs.* severe RFI group; ‡: P<0.001, *vs.* severe RFI group. RFI: renal function impairment.

and mild RFI groups. AQP1-4 protein expression in the mild RFI group was also significantly reduced compared with the control kidneys (Table).

The cellular distribution of AQP1-4 in the human renal controls is shown in Fig. 3. AQP1 was located to basolateral and apical membranes of the proximal tubules and AQP1 staining was prominent in all viable proximal tubules in normal kidneys (Fig. 3A). It was absent in other parts of the nephron and in the collecting duct. In both mild RFI and severe RFI groups, there was an apparent reduction of AQP1 staining in the proximal tubules (Fig. 3B and C). The expression of AQP2 was located at the apical membrane of collecting duct principal cells in normal kidneys (Fig. 3D), whereas AQP3 and AQP4 were located at the basolateral membrane of the collecting duct principal cells (Fig. 3G and J). As demonstrated, the protein abundance of AQP2-4 was reduced in the hydronephrotic kidney. Importantly, the labeling was more reduced in the kidneys of the severe RFI group (Fig. 3F, I, L) than in those of the mild RFI group (Fig. 3E, H, K).

Discussion

It has been reported that AQP1-4 plays critical roles for transepithelial water transport in the proximal tubules, descending thin limb of Henle and the collecting duct, and an intact expression is important for normal urinary concentrating capacity.[11] Animal study demonstrated that the decreased expression of AQP1-4 is proportional to the decrease of renal function.[1-4]

In the present study we collected more kidney samples and found a relationship between the expression of AQP1-4 and the RFI evaluated by ^{99m}Tc-DTPA renal dynamic imaging.

We chose the shape of TAC and TOP in ^{99m}Tc-DTPA renal dynamic imaging to evaluate and classify renal function impairment degree in different hydronephrosis cases, which was demonstrated by Elgazzar et al[10] early in 1990. Clinically, we found the shape of TAC was typical in hydronephrotic cases with different degrees of RFI which could be easily identified, and TOP was always more than 18 minutes in hydronephrotic cases with severe renal function impairment. We also found that the drainage half-time on ^{99m}Tc-DTPA renal dynamic imaging of all hydronephrotic cases was more than 20 minutes.

In the present study, we further examined whether progressive renal deterioration could be related to altered regulation of AQPs in the obstructed kidneys. Semiquantitative immunoblotting of obstructed kidneys demonstrated that AQP2 protein expression was downregulated, as reported elsewhere.[5] This was also in accordance with the immunocytochemical study demonstrating a weaker labeling of AQP2 in the apical parts of the collecting duct principal cells. In parallel, renal function also decreased in obstructed kidneys, suggesting a functional association between AQP2 downregulation and renal function impairment. AQP2 is the apical water channel of the principal cells and is the chief target for regulation of collecting duct water permeability by vasopressin.[12] The urinary concentrating process depends on the coordinated

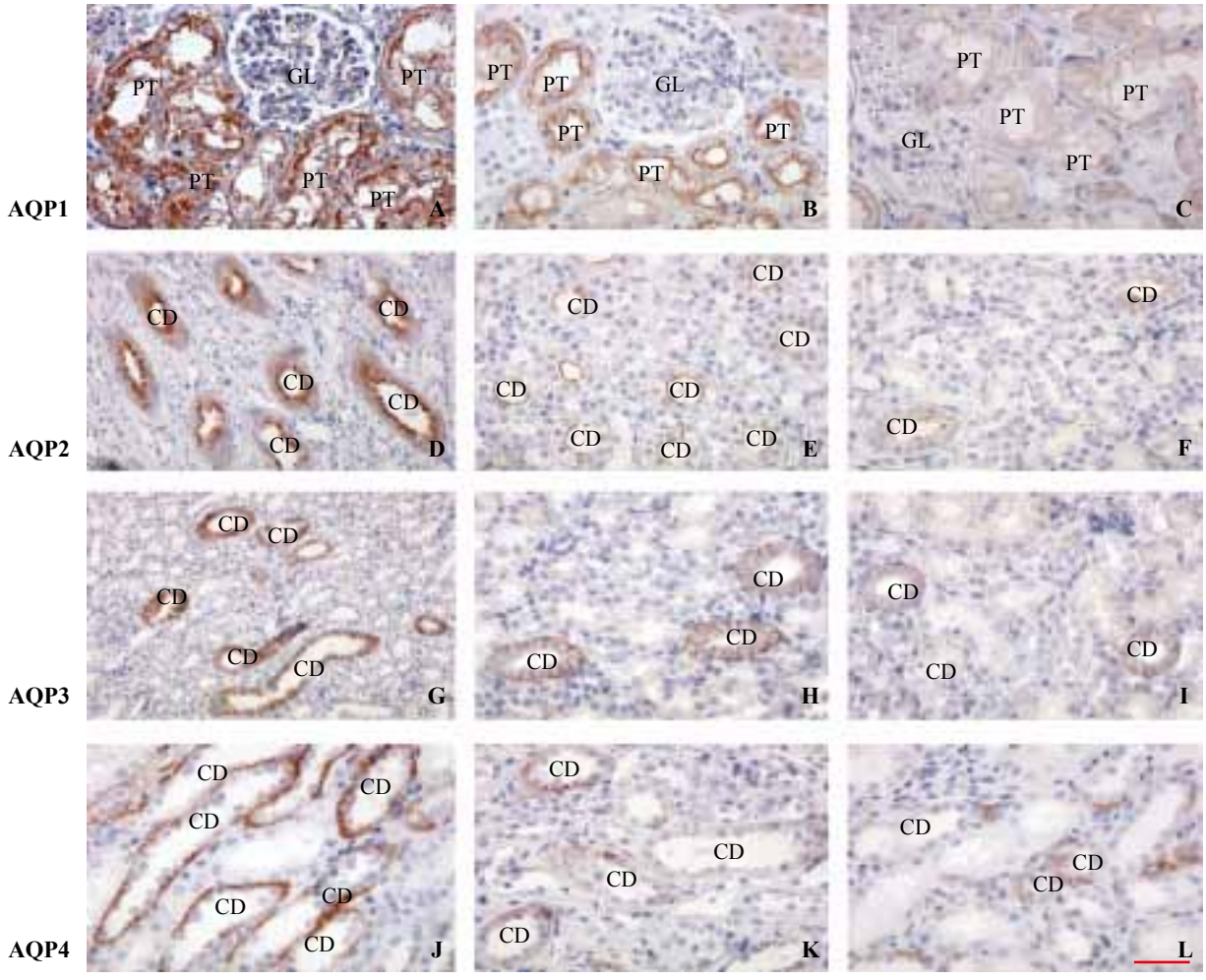

Fig. 3. Immunohistochemistry for AQP1-4 in renal control and of kidney from patients with mild RFI group and severe RFI group. Bar = 100 μm. AQP1-4 localization in the control kidney (**A**, **D**, **G**, **J**), and mild RFI group (**B**, **E**, **H**, **K**) and severe RFI group (**C**, **F**, **I**, **L**) as detected by immunostaining with horseradish peroxidase, respectively (original magnification × 40). PT: proximal tubules; GL: glomerulus; CD: collecting duct; AQP1-4: aquaporins 1-4; RFI: renal function impairment.

function of the loop of Henle and the collecting duct. The thick ascending limb of the loop of Henle powers the countercurrent multiplier process responsible for the generation of a corticomedullary osmotic gradient, whereas the collecting ducts, under the control of vasopressin, allow variable degrees of osmotic equilibration, resulting in a variable amount of excreted water and a reciprocal relationship between urinary flow and urinary osmolality.[13] The changed expression of AQP2 may play an important role in the impairment of renal function during obstruction.

AQP3 and AQP4 represent exit pathways of water through the basolateral membrane in the collecting duct principal cells. It is well known that AQP3 knockout mice are able to generate only partially concentrated urine after water deprivation.[14] The mechanisms underlying the regulation of AQP3 expression are presently not well understood. There is clear evidence that AQP3 regulation is linked to changes in vasopressin levels and water balance. AQP4 is responsible for the majority of basolateral membrane water movement in the inner medullary collecting duct, but AQP4 knockout mice only demonstrate a mild defect in urinary concentrating ability.[15] The AQP3/AQP4 double-knockout mice had a greater impairment of urinary concentrating ability than the AQP3 single-knockout mice.[16] Our results also demonstrated downregulation of AQP3 and AQP4 in obstructed kidneys together with a parallel impairment of renal function after obstruction. The changed expression of AQP2-4 may play an important role in the decrease of renal concentrating ability during obstruction.

We also found that AQP1 expressed in the proximal tubules, descending thin limbs and vasa recta was markedly decreased in both mild RFI group and severe RFI group compared with the renal controls. It has

been documented that a significant amount of AQP1 is present in the renal proximal tubules. This nephron segment, in conjunction with the descending thin limbs, is responsible for an 80%-90% fluid reabsorption of glomerular filtrate.[17] AQP1 expression changes in proximal tubule fluid transport may have significant effects on the urinary concentrating mechanism by altering flow rates of tubule fluid delivery to the thick ascending limbs and collecting ducts. Therefore, impairment of proximal tubule function, demonstrated by a decline in AQP1 abundance, could contribute to the changes in urinary flow. Decreased AQP1 expression may be associated with the impairment of renal reabsorption and concentrating function during obstruction.

Diuretic renography with DTPA provides a noninvasive means of differentiating obstructive from nonobstructive hydronephrosis and calculating differential renal function, which reflects the relative ability of the kidney to extract the radiotracer from blood.[18] Management of CH patients is generally guided by renal function, determined as differential function from the ^{99m}Tc-DTPA renogram, and not by the drainage or the response to a diuretic. A major and anticipated role of AQPs in the kidney is in water transport across kidney tubules and vasa recta for the formation of concentrated urine in the antidiuretic kidney. The results of the present study indicates that there is a relationship between AQPs expression alteration and renal function impairment during obstruction in pediatric CH patients.

In the present study, the study on the contralateral kidney was absent, because the contralateral kidney was intact during surgery. The contralateral kidney demonstrated increased reabsorption and excretion of water and solutes during ureteral obstruction, which takes place to compensate for the impaired excretion from the obstructed kidney.[19] The very extensive downregulation of AQP1-4 protein has been found in the obstructed kidneys and unchanged expression levels of AQP2-4 in the nonobstructed kidneys of the same animals are consistent with the view, which emphasizes that local, intrarenal factors play a major role in the induction of downregulation.[19] However, systemic factors also appear to be involved, because there was a significant decrease in AQP1 protein levels in nonobstructed kidneys compared with sham-operated controls. Because of the challenge of sample collection from the contralateral kidney, the situation of the AQP1-4 expression in the contralateral kidney in patients with UPJO is at present unknown.

The limitation of the present study is immunohistochemistry method, which is affected by multiple factors and cannot localize AQP1-4 expression in the renal tubular epithelial cell accurately. Moreover, a control gene should be used during the immunohistochemistry. Another point is the quantity of renal sample from the obstructed kidney, which is relatively less and does not allow us to investigate AQP1-4 expression in the cortex, inner medullary and inner stripe of the outer medulla of the kidney.

In conclusion, the present study demonstrated a significant downregulation of AQP1-4 protein in the mild RFI group compared with the normal control group, and a further significant decrease in the severe RFI group compared with the mild RFI group, which may at least in part account for different degree renal function impairment in human congenital hydronephrosis caused by UPJO. However, the mechanism involved in this relationship needs to be investigated in the future.

Acknowledgments

We are thankful to Prof. Robert Levin, Albany College of Pharmacy, Albany, NY, USA for his helpful review.

Funding: This study was supported by the National Natural Science Foundation of China (NSFC) (grant number: 30571931), the Youth Innovation Fund of the First Affiliated Hospital of Zhengzhou University and Special Research Fund for the Doctoral Program of Colleges of Ministry of Education (No. 20114101120010).

Ethical approval: The enrollment of patients to the study was performed after permission of the First Affiliated Hospital of Zhengzhou University Ethical Committee.

Competing interest: The authors declare no conflicts of interest.

Contributors: Li ZZ drafted the paper. All authors contributed to the intellectual content and the final version. Wen JG is the guarantor.

References

1 Jensen AM, Li C, Praetorius HA, Nørregaard R, Frische S, Knepper MA, et al. Angiotensin II mediates downregulation of aquaporin water channels and key renal sodium transporters in response to urinary tract obstruction. Am J Physiol Renal Physiol 2006;291:F1021-1032.

2 Li C, Shi Y, Wang W, Sardeli C, Kwon TH, Thomsen K, et al. alpha-MSH prevents impairment in renal function and dysregulation of AQPs and Na-K-ATPase in rats with bilateral ureteral obstruction. Am J Physiol Renal Physiol 2006; 290:F384-396.

3 Topcu SO, Nørregaard R, Pedersen M, Wang G, Jørgensen TM, Frøkiær J. Regulation of aquaporins and sodium transporter proteins in the solitary kidney in response to partial ureteral obstruction in neonatal rats. Urol Int 2011;87:94-104.

4 Stødkilde L, Nørregaard R, Fenton RA, Wang G, Knepper MA, Frøkiær J. Bilateral ureteral obstruction induces early downregulation and redistribution of AQP2 and phosphorylated

AQP2. Am J Physiol Renal Physiol 2011;301:F226-235.
5 Wen JG, Li ZZ, Zhang H, Wang Y, Wang G, Wang Q, et al. Expression of renal aquaporins is down-regulated in children with congenital hydronephrosis. Scand J Urol Nephrol 2009;43:486-493.
6 Koff SA, Campbell KD. The nonoperative management of unilateral neonatal hydronephrosis: natural history of poorly functioning kidneys. J Urol 1994;152:593-595.
7 Oh SJ, Moon DH, Kang W, Park YS, Park T, Kim KS. Supranormal differential renal function is real but may be pathological: assessment by 99mtechnetium mercaptoacetyltriglycine renal scan of congenital unilateral hydronephrosis. J Urol 2001;165:2300-2304.
8 Braren V, Versage PN, Touya JJ, Brill AB, Goddard J, Rhamy RK. Radioisotopic determination of glomerular filtration rate. J Urol 1979;121:145-147.
9 Gutte H, Møller ML, Pfeifer AK, Thorup J, Borgwardt L, Borgwardt L, et al. Estimating GFR in children with 99mTc-DTPA renography: a comparison with single-sample 51Cr-EDTA clearance. Clin Physiol Funct Imaging 2010;30:169-174.
10 Elgazzar AH, Bahar RH, Abu-Zidan FM, Francis IM, Sabha M, Kouris K, et al. Experimental complete ureteric occlusion in sheep: radionuclide renography and histopathologic findings. Eur J Nucl Med 1990;17:230-233.
11 Verkman AS. Knock-out models reveal new aquaporin functions. Handb Exp Pharmacol 2009;(190):359-381.
12 Eto K, Noda Y, Horikawa S, Uchida S, Sasaki S. Phosphorylation of aquaporin-2 regulates its water permeability. J Biol Chem 2010;285:40777-40784.
13 Boone M, Deen PM. Physiology and pathophysiology of the vasopressin-regulated renal water reabsorption. Pflugers Arch 2008;456:1005-1024.
14 Tradtrantip L, Tajima M, Li L, Verkman AS. Aquaporin water channels in transepithelial fluid transport. J Med Invest 2009;56 Suppl:179-184.
15 Chou CL, Ma T, Yang B, Knepper MA, Knepper MA, Verkman AS. Fourfold reduction of water permeability in inner medullary collecting duct of aquaporin-4 knockout mice. Am J Physiol Cell Physiol 1998;274:C549-C554.
16 Kim SW, Gresz V, Rojek A, Wang W, Verkman AS, Frøkiaer J, et al. Decreased expression of AQP2 and AQP4 water channels and Na, K-ATPase in kidney collecting duct in AQP3 null mice. Biol Cell 2005;97:765-778.
17 Bouley R, Palomino Z, Tang SS, Nunes P, Kobori H, Lu HA, et al. Angiotensin II and hypertonicity modulate proximal tubular aquaporin 1 expression. Am J Physiol Renal Physiol 2009;297:F1575-1586.
18 Renjen P, Bellah R, Hellinger JC, Darge K. Pediatric urologic advanced imaging: techniques and applications. Urol Clin North Am 2010;37:307-318.
19 Li C, Wang W, Knepper MA, Nielsen S, Frøkiaer J. Downregulation of renal aquaporins in response to unilateral ureteral obstruction. Am J Physiol Renal Physiol 2003;284: F1066-1069.

Received August 20, 2011
Accepted after revision April 23, 2012